Age, extent and carbon storage of the central Congo Basin peatland complex

Greta C. Dargie[1,2]*, Simon L. Lewis[1,2]*, Ian T. Lawson[3], Edward T. A. Mitchard[4], Susan E. Page[5], Yannick E. Bocko[6] & Suspense A. Ifo[6]

Peatlands are carbon-rich ecosystems that cover just three per cent of Earth's land surface[1], but store one-third of soil carbon[2]. Peat soils are formed by the build-up of partially decomposed organic matter under waterlogged anoxic conditions. Most peat is found in cool climatic regions where unimpeded decomposition is slower, but deposits are also found under some tropical swamp forests[2,3]. Here we present field measurements from one of the world's most extensive regions of swamp forest, the Cuvette Centrale depression in the central Congo Basin[4]. We find extensive peat deposits beneath the swamp forest vegetation (peat defined as material with an organic matter content of at least 65 per cent to a depth of at least 0.3 metres). Radiocarbon dates indicate that peat began accumulating from about 10,600 years ago, coincident with the onset of more humid conditions in central Africa at the beginning of the Holocene[5]. The peatlands occupy large interfluvial basins, and seem to be largely rain-fed and ombrotrophic-like (of low nutrient status) systems. Although the peat layer is relatively shallow (with a maximum depth of 5.9 metres and a median depth of 2.0 metres), by combining *in situ* and remotely sensed data, we estimate the area of peat to be approximately 145,500 square kilometres (95 per cent confidence interval of 131,900–156,400 square kilometres), making the Cuvette Centrale the most extensive peatland complex in the tropics. This area is more than five times the maximum possible area reported for the Congo Basin in a recent synthesis of pantropical peat extent[2]. We estimate that the peatlands store approximately 30.6 petagrams (30.6 × 10^{15} grams) of carbon belowground (95 per cent confidence interval of 6.3–46.8 petagrams of carbon)—a quantity that is similar to the above-ground carbon stocks of the tropical forests of the entire Congo Basin[6]. Our result for the Cuvette Centrale increases the best estimate of global tropical peatland carbon stocks by 36 per cent, to 104.7 petagrams of carbon (minimum estimate of 69.6 petagrams of carbon; maximum estimate of 129.8 petagrams of carbon[2]). This stored carbon is vulnerable to land-use change and any future reduction in precipitation[7,8].

The Congo Basin drains an area of approximately 3.7 × 10^{6} km[2], within which lies a central shallow depression overlaid by swamp forest, known as the Cuvette Centrale[9]. Over this region, the Congo River drops just 115 m over 1,740 km, with year-round waterlogging[9]; we therefore hypothesized that this wetland—the second largest in the tropics—might contain extensive peat deposits. A few grey literature sources since the 1950s briefly mention peat occurring in the central Congo Basin, but geolocations or other details were not reported[10–13]. Recently published estimates of tropical peatland area and carbon storage still rely on this scant, unverifiable information[2,14]. Therefore, here we first assess whether the Cuvette Centrale contains substantial peat deposits, and then estimate the extent and total carbon storage of the peatlands we identify.

We combined a digital elevation model (DEM; from the Shuttle Radar Topography Mission, SRTM) to exclude high ground and steep slopes, radar backscatter (from the Advanced Land Observation Satellite Phased Array type L-band Synthetic Aperture Radar, ALOS PALSAR) to detect standing surface water under forest, and optical data (from Landsat Enhanced Thematic Mapper, ETM+) to categorize likely swamp vegetation, to identify areas to prospect for peat (Extended Data Table 1). We identified nine transects (2.5–20 km long) within an approximately 40,000 km[2] area of northern Republic of the Congo (ROC), each traversing more than one vegetation type within waterlogged regions, and collectively spanning the range of non-waterlogged vegetation types (Fig. 1). We confirmed the presence of peat (defined as deposits at least 0.3 m deep with an organic matter content of at least 65%) in all eight areas in which we expected to find it: four perpendicular to a low-nutrient black-water river, pH 3.8; three perpendicular to a more nutrient-rich white-water river, pH 7.4, which has high banks and probably does not contribute water to the swamp; and one transect at the midpoint of the two rivers. We also confirmed the absence of peat in abandoned channels of the white-water river where higher nutrient levels probably increase dry-season decomposition, thereby preventing peat formation.

Peat thickness, measured at least every 250 m along each transect, increased with increasing distance from peatland edges, to a maximum depth of 5.9 m near the mid-point between the two rivers (mean depth, 2.4 m; 95% confidence interval (CI), 2.2–2.6 m; $n = 211$; Fig. 2). These peat thicknesses are shallower than in many other parts of the tropics (Table 1). Radiocarbon dating of basal peat samples returned ages ranging from 10,554 to 7,137 cal yr BP (calibrated ^{14}C years before present, where 'present' is defined to be 1950; at 2σ; Extended Data Table 2). These dates are consistent with peat initiation and carbon accumulation being linked to a well-documented increase in humidity across the Congo Basin at the onset of the African Humid Period during the early Holocene (between about 11,000 and 8,000 cal yr BP)[5] (Extended Data Table 3). Additional radiocarbon dates show 0.57–0.80 m of peat accumulation over the past 1,464–2,623 cal yr BP (Extended Data Table 2), indicating that peat has continued to accumulate since the end of the African Humid Period at the low latitude of the Cuvette Centrale swamps (about 3,000 cal yr BP)[15].

The waterlogging that inhibits the decay of organic matter may be due to poor drainage and high rainfall (about 1,700 mm yr^{-1}), and/or overbank flooding by rivers. One year of continuous measurements of the peatland water table across four of the transects (Fig. 1) showed no evidence of flood waves (Extended Data Fig. 1; a flood wave was recorded using a similar sensor in a Peruvian peatland[16]). Recorded increases in the water table were largely consistent with the rainfall record estimated from the Tropical Rainfall Monitoring Mission (product 3B42; Extended Data Fig. 1). Furthermore, the calcium concentration within surface peats is low (0.3 g kg^{-1}), as is

[1]School of Geography, University of Leeds, Leeds LS2 9JT, UK. [2]Department of Geography, University College London, London WC1E 6BT, UK. [3]Department of Geography and Sustainable Development, University of St Andrews, St Andrews KY16 9AL, UK. [4]School of GeoSciences, University of Edinburgh, Edinburgh EH9 3FF, UK. [5]Department of Geography, University of Leicester, Leicester LE1 7RH, UK. [6]Faculté des Sciences et Techniques, Université Marien Ngouabi, Brazzaville, Republic of the Congo.
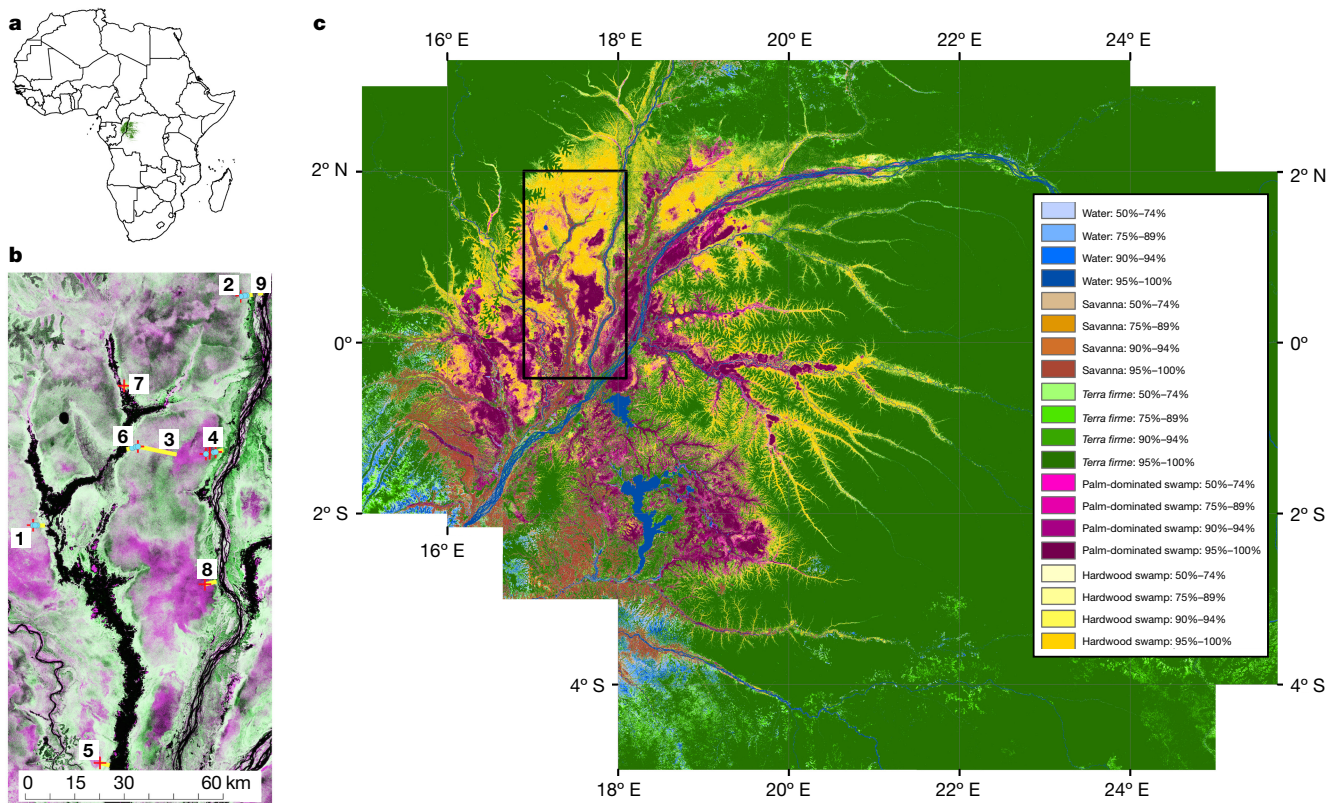*These authors contributed equally to this work.

Figure 1 | Location of the Cuvette Centrale wetlands, study sites and our peatland probability map. a, Location of the Cuvette Centrale wetland (shaded green) within the African continent. **b**, ALOS PALSAR radar imagery showing the transect locations (yellow): 1, Bondoki; 2, Bondzale; 3, Center; 4, Ekolongouma; 5, Ekondzo; 6, Itanga; 7, Makodi; 8, Mbala; 9, Moungouma. The locations of the basal peat samples (red) and water table measurements (blue) are also shown. In black, on the left is the meandering black-water Likouala-aux-herbes River; on the right is the straighter white-water Ubangi River. Green shading indicates the vegetation density: dark areas are savannas or water and bright green areas have tree-dominated vegetation (from cross-polarized horizontally transmitted, vertically received (HV) radar signal data). Magenta shading indicates palm-dominated swamp, owing to the strong double bounce from stems and wet soil (from single-polarized horizontally transmitted, horizontally received (HH) radar signal data). **c**, Probability map of vegetation types derived from 1,000 runs of a maximum likelihood classification using eight remote sensing products (three ALOS PALSAR; two SRTM-derived variables; three Landsat ETM+ bands) and jack-knifed selections of training data. The black box shows the area in **b**. Field observations show that peat underlies both hardwood tree- and palm-dominated swamp forest.

pH (3.2), similar to other ombrotrophic rainwater-fed tropical peatlands, within which the calcium concentration is typically less than $0.4\,\mathrm{g\,kg^{-1}}$ (refs 17, 18); by contrast, in minerotrophic river-fed peatlands, the calcium concentration is typically $1–10\,\mathrm{g\,kg^{-1}}$ (refs 16, 17). We also observed peatland inundation while river levels were still well below their banks. Although supra-annual river flooding cannot be excluded[19], the peatlands of the Cuvette Centrale can be considered ombrotrophic-like peatlands, owing to their low-nutrient status and heavily rainwater-dependent water tables. This classification is consistent with previous satellite-only studies that suggested that these wetlands are largely hydrologically independent from regional rivers[20,21], and with our radiocarbon dates that suggest that peat accumulation began with an increase in regional precipitation.

Our transect sampling shows that peat is consistently found under two common vegetation types: hardwood swamp forest (in which *Uapaca paludosa*, *Carapa procera* and *Xylopia rubescens* are common) and a palm-dominated (*Raphia laurentii*) swamp forest. Peat was also usually found under another, much rarer palm-dominated (*Raphia hookeri*) swamp forest that occupies abandoned river channels. Peat was not found beneath *terra firme* forest, seasonally flooded forest or savanna (Extended Data Table 4). We used these peat–vegetation associations to estimate the extent of peatlands within the Cuvette Centrale, via remotely sensed mapping of the extent of hardwood and palm-dominated swamps. Field ground-truth points of land-cover classes (516 in total), including hardwood swamp approximately 300 km

from our main study region, were used to train a maximum likelihood classification derived from eight remotely sensed data layers (simple and cross-polarizations and their ratio from ALOS PALSAR; slope and elevation from the SRTM DEM; and Landsat ETM+ bands 3, 4 and 5; Extended Data Fig. 2, Extended Data Table 5). Running the classification 1,000 times, each time using a random two-thirds sample of ground-truth points as training data, generated a peatland probability map with a median area of $145{,}500\,\mathrm{km^2}$ (Fig. 1; mean, $145{,}200\,\mathrm{km^2}$; 95% CI, $131{,}900–156{,}400\,\mathrm{km^2}$; median overall classification accuracy against independent test data, 88%; Extended Data Table 6). This area is greater than five times the 'maximum possible' area reported for this region in a recent synthesis of pantropical peat land extent[2]. A comparison of our estimated area of swamp vegetation that overlies peat with other remotely sensed estimates of the total regional wetland extent, including seasonal wetlands[22], suggests that peatlands account for around 40% of the total extent of the Cuvette Centrale wetlands.

Although further measurements are required to improve our initial estimate of the area of peat within the Cuvette Centrale, it is very likely to be the largest peatland complex in the tropics. Peatlands on the tropical Asian islands of New Guinea, Borneo and Sumatra cover $101{,}000\,\mathrm{km^2}$, $73{,}000\,\mathrm{km^2}$ and $69{,}000\,\mathrm{km^2}$, respectively, but today about 30%, 40% and 50% of these areas have undergone land-use change and drainage[23]. Each of these estimates is below our lower confidence interval of peat extent within the Cuvette Centrale.
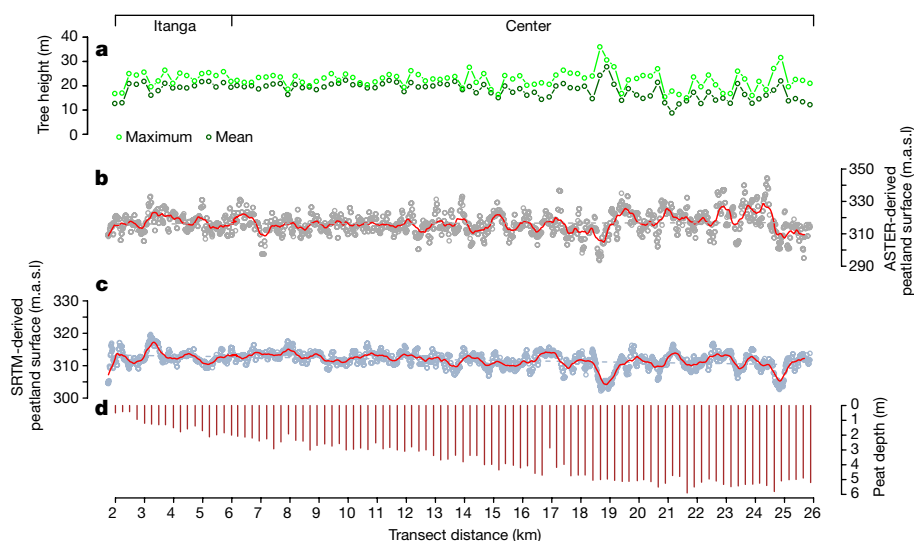
Figure 2 | Tree height, peatland surface and peat depth along 24 km of transects extending from the peatland edge to the interfluvial centre.
a, Maximum (light green) and mean (dark green) tree height measured *in situ*. **b**, ASTER-derived peatland surface (grey circles; ASTER DEM minus maximum tree height), linear trend line (grey dashed line; slope, 0.04 m km^{-1}; 95% CI, 0–0.08 m km^{-1}; not significant, $P > 0.05$) and a running mean of the estimated peatland surface using 20 data points before and 20 points after the focal data point (red line). **c**, SRTM-derived estimated peatland surface (light blue circles; SRTM DEM minus mean tree height), linear trend line (blue dashed line; slope, −0.12 m km^{-1}; 95% CI, −0.14 m km^{-1} to −0.11 m km^{-1}; $P < 0.001$) and running mean (red line). **d**, Peat depth, measured *in situ*, every 250 m (in brown). The two transects—Itanga (perpendicular to the Likouala-aux-herbes River; number 6 in Fig. 1b) and Center (running from the end of the Itanga transect to the mid-point of the interfluvial region between the Likouala-aux-herbes and Ubangui rivers; number 3 in Fig. 1b)—are contiguous, but follow different bearings (N 77° E and S 78° E, respectively). m.a.s.l., metres above sea level.

Combining the estimates of peatland area with our measurements of peat depth, bulk density and carbon concentration, using a resampling approach, we find that the median total peat carbon storage within the Cuvette Centrale is 30.6 petagrams of carbon (Pg C; mean, 29.8 Pg C; 95% CI, 6.3–46.8 Pg C; Extended Data Figs 3, 4). Uncertainty, although absolutely large, is proportionally smaller than initial estimates of other extensive peatlands[3]. Additional measurements of peat depth, guided by our map, should reduce the uncertainty on our first estimate. Our *in situ* vegetation sample plots show that the amount of carbon stored in the peat is much greater than that stored in the living vegetation overlying the peatland (median, 1.4 Pg C; 95% CI, 0.6–2.5 Pg C; $n = 60$). Total below-ground carbon storage is likely to be greater than peat-only estimates suggest, because a layer of organic-matter-rich and carbon-rich material occurs beneath the true peat, but has an organic matter content of less than 65% (Extended Data Fig. 3).

The most recent synthesis of tropical peat carbon storage[2] suggests that total peat carbon storage across the African continent is 7 Pg C, which rises to 34.4 Pg C after taking into account our new Cuvette Centrale estimate. Total tropical peat carbon stocks were also estimated, at 89 Pg (ref. 2), which, after accounting for losses from extensive ongoing land-use change and peat fires in Asia in the approximately 23 years since the data was collected[2] (around 0.5 Pg C yr^{-1}; ref. 24), and combining with our new Cuvette Centrale data, yields a total contemporary tropical peat carbon stock of 104.7 Pg C (with a minimum estimate of 69.6 Pg C and a maximum of 129.8 Pg C; see ref. 2). Approximately 29% of the total tropical peat carbon stock is found within the Cuvette Centrale. In terms of both peat area and peat carbon stocks, the Democratic Republic of the Congo (DRC; 90,800 km^2 of peat; 19.1 Pg C) and ROC (54,700 km^2 of peat; 11.5 Pg C) become the second and third most important countries in the tropics for peat areas and carbon stocks, after Indonesia[2]. Globally they are the fifth and ninth most important, respectively, for peat area, and the fifth and sixth most important in terms of carbon stocks[25]; together they account for approximately 5% of the estimated global peat carbon stock[2]. Translating the long-term carbon sink in peat into contemporary CO_2 fluxes is challenging, requiring an integrated multi-sensor monitoring programme. Combining contemporary CO_2 flux estimates with CH_4

emissions (which are large, but poorly constrained[26]) would then improve our understanding of the role of the wetland within the global carbon cycle and climate system.

The world's three major regions of lowland tropical peat—in the Cuvette Centrale, the tropical islands of Asia, and Western Amazonia—appear to strongly differ (Table 1). Surface topography assessments, using either SRTM or ASTER (Advanced Spaceborne Thermal Emission and Reflection Radiometer), did not reveal clear domes, where the peat surface increases from the edge to the interior of the peatland. Such domes are expected in poorly draining rain-fed systems ('raised bogs')[27], as seen in many, but not all, Western Amazonian[17] and tropical Asian[18,28] peatlands (Fig. 2). However, our surface topography detection limits are probably 2–3 m, and independent satellite altimetry data suggests that water levels in the interfluvial wetlands are always 0.5–3 m higher than those in adjacent rivers[26], consistent with very small domes. Overall, our results imply that, within the Cuvette Centrale, large-scale shallow interfluvial basins have filled with peat, which gradually increases in thickness away from the river margins (Fig. 2). This peat accumulated slowly, on average, over the Holocene (Table 1). By contrast, in a typical tropical Asian system, high precipitation and the persistence of climatic conditions suitable for peat accumulation since the early Holocene, and often before the Last Glacial Maximum, has allowed peat to accumulate to greater thickness and form clear domes[29,30]. Lowland Western Amazonia differs again: high precipitation levels during the Holocene have permitted relatively rapid peat accumulation since at least 8,900 cal yr BP in places, and domes to form, but the location of peat on dynamic river floodplains means that these peatlands rarely survive long enough to accumulate peat to a great thickness[31]. The differences between the lowland tropical peatlands extend to peat properties. Cuvette Centrale peat has much higher bulk density and slightly higher carbon concentration than does typical peat in the other two regions, probably reflecting greater decomposition in the Cuvette Centrale, thereby increasing carbon storage per unit volume of peat (Table 1).

The Cuvette Centrale peatlands are relatively undisturbed at present, owing to difficult access and distance from markets. However, they face two threats: changes in land-use, particularly drainage for

Table 1 | Properties of tropical lowland African, Asian and American peatlands

Region	Peatland area (km²)	Basal peat age (cal kyr BP)	Peat depth (m)	Peat bulk density (g cm⁻³)	Carbon (%)	Carbon density (g C cm⁻³)	Peat accumulation rate (mm yr⁻¹)	LORCA (g C m⁻² yr⁻¹)
Cuvette Centrale, Central Congo Basin	145,500 (131,900–156,400)	8.9 ± 1.2 (10.6*)	2.4 ± 1.6† (5.9)	0.19 ± 0.06§ (0.1, 0.32)	59 ± 3# (53, 63)	0.11 ± 0.028** (0.06, 0.15)	0.21 ± 0.05 (0.16, 0.29)	23.9 ± 5.8 (18.3, 33.1)
Central Kalimantan, Borneo[28–30,33]	30,100 (NR)	14.1 ± 7.0 (~26.0)	4.7 ± 0.9 (9.4‡)	0.11 ± 0.03‖ (NR)	57 ± 2‖ (NR)	0.061 ± 0.015 (0.046, 0.075)	0.54 (NR)	31.3 (16.6, 73.2)
Pastaza–Marañón Basin, western Amazonia[3,16,31]	35,600 (33,500–37,700)	3.5 ± 2.8 (8.9)	2.5 ± 0.7 (7.5‡)	0.11 ± 0.06¶ (0.05, 0.24)	46 ± 8* (30, 54)	0.033 ± 0.011 (0.021, 0.050)	1.74 ± 0.72 (0.72, 2.56)	52 ± 22 (36, 85)

For peatland area, the best estimate is given, with the 95% CI in parentheses. All other values are mean ± 1 s.d., with the greatest age (basal peat age), maximum (peat depth), or minimum and maximum (all others) values in parentheses. The values for the central Congo Basin are from this study. NR, not reported; LORCA, long-term rate of carbon accumulation.
*The deepest approximately 0.25 m of peat of the deepest and oldest basal sample could not be recovered from the ground, but the average peat accumulation rate for this core indicates that peat initiation might be about 980 yr earlier than stated, at around 11,500 cal yr BP (Extended Data Tables 2, 3).
†Median, 2.0 m; $n = 211$.
‡Greater depth values have been reported from other regions within southeast Asia and Amazonia[2].
§Median, 0.19 g cm⁻³; $n = 44$ cores; 372 samples in total.
‖$n = 20$ cores, 173 samples in total.
¶$n = 9$ cores; 134 samples in total.
#Median, 59%; $n = 12$ cores; 181 samples in total.
*$n = 9$ cores; 101 samples in total.
**Median, 0.10 g C cm⁻³; 12 cores; 181 samples.

agricultural use, as is occurring extensively across tropical Asia; and a regional reduction in precipitation via a changing climate, which may already be occurring[32]. Although modelled projections of central African rainfall are not consistent, some suggest declining annual precipitation[7] and more intense dry seasons[8]. The existence of large carbon stocks in peat—potentially equivalent to 20 years of current fossil fuel emissions from the United States of America—increases the importance of improving climate model projections for central Africa, a long neglected region.

The swamps of the Cuvette Centrale are refuges for remaining megafauna populations, including lowland gorillas and forest elephants. Our findings suggest that they are also the world's most extensive tropical peatland complex and among the most carbon-dense ecosystems on Earth, storing on average 2,186 Mg C ha⁻¹. The existence of such large and previously unquantified components of the national carbon stocks of both ROC and DRC provides an additional imperative for governments, alongside conservation, development and scientific communities, to work with the people of the Cuvette Centrale to pursue development pathways that will radically improve local livelihoods and welfare without compromising the integrity of this globally significant region of Earth.

1. Rydin, H. & Jeglum, J. K. *The Biology of Peatlands* 230–233 (Oxford Univ. Press, 2006).
2. Page, S. E., Rieley, J. O. & Banks, C. J. Global and regional importance of the tropical peatland carbon pool. *Glob. Change Biol.* **17,** 798–818 (2011).
3. Draper, F. C. *et al.* The distribution and amount of carbon in the largest peatland complex in Amazonia. *Environ. Res. Lett.* **9,** 124017 (2014).
4. Keddy, P. A. *et al.* Wet and wonderful: the world's largest wetlands are conservation priorities. *Bioscience* **59,** 39–51 (2009).
5. Schefuß, E., Schouten, S. & Schneider, R. R. Climatic controls on central African hydrology during the past 20,000 years. *Nature* **437,** 1003–1006 (2005).
6. Verhegghen, A., Mayaux, P., de Wasseige, C. & Defourny, P. Mapping Congo Basin vegetation types from 300 m and 1 km multi-sensor time series for carbon stocks and forest areas estimation. *Biogeosciences* **9,** 5061–5079 (2012).
7. Haensler, A., Saeed, F. & Jacob, D. Assessing the robustness of projected precipitation changes over central Africa on the basis of a multitude of global and regional climate projections. *Clim. Change* **121,** 349–363 (2013).
8. James, R., Washington, R. & Rowell, D. P. Implications of global warming for the climate of African rainforests. *Phil. Trans. R. Soc. B* **368,** (2013).
9. Hughes, R. H. & Hughes, J. S. *A Directory of African Wetlands* 493, 547–557 (IUCN, 1992).
10. Bouillenne, R., Moureau, J. & Deuse, P. *Esquisse écologique des faciès forestiers et marécageux des bords du lac Tumba (Domaine de l'I. R. S. A. C., Mabali, Congo Belge)* (Académie royale des Sciences Coloniales, 1955).
11. Évrard, C. *Recherches écologiques sur le peuplement forestier des sols hydromorphes de la Cuvette centrale congolaise* 71, 73, 194 (INEAC, 1968).
12. Bord na Móna. *Fuel Peat in Developing Countries.* World Bank Technical Paper No. 41 (The World Bank, 1985).
13. Markov, V. D., Olunin, A. S., Ospennikova, L. A., Skobeeva, E. I. & Khoroshev, P. I. *World Peat Resources* (Nedra, 1988).
14. Joosten, H., Tapio-Biström, M. L. & Tol, S. *Peatlands - Guidance for Climate Change Mitigation Through Conservation, Rehabilitation and Sustainable Use.* (FAO and Wetlands International, 2012).
15. Shanahan, T. M. *et al.* The time-transgressive termination of the African Humid Period. *Nat. Geosci.* **8,** 140–144 (2015).
16. Lawson, I. T., Jones, T. D., Kelly, T. J., Coronado, E. N. H. & Roucoux, K. H. The geochemistry of Amazonian peats. *Wetlands* **34,** 905–915 (2014).
17. Lähteenoja, O. & Page, S. High diversity of tropical peatland ecosystem types in the Pastaza-Marañón basin, Peruvian Amazonia. *J. Geophys. Res. Biogeosci.* **116,** G02025 (2011).
18. Page, S. E., Rieley, J. O., Shotyk, O. W. & Weiss, D. Interdependence of peat and vegetation in a tropical peat swamp forest. *Phil. Trans. R. Soc. Lond. B* **354,** 1885–1897 (1999).
19. Runge, J. & Nguimalet, C. R. Physiogeographic features of the Oubangui catchment and environmental trends reflected in discharge and floods at Bangui 1911–1999, Central African Republic. *Geomorphology* **70,** 311–324 (2005).
20. Lee, H. *et al.* Characterization of terrestrial water dynamics in the Congo Basin using GRACE and satellite radar altimetry. *Remote Sens. Environ.* **115,** 3530–3538 (2011).
21. Jung, H. C. *et al.* Characterization of complex fluvial systems using remote sensing of spatial and temporal water level variations in the Amazon, Congo, and Brahmaputra Rivers. *Earth Surf. Process. Landf.* **35,** 294–304 (2010).
22. Bwangoy, J.-R. B., Hansen, M. C., Roy, D. P., De Grandi, G. & Justice, C. O. Wetland mapping in the Congo Basin using optical and radar remotely sensed data and derived topographical indices. *Remote Sens. Environ.* **114,** 73–86 (2010).
23. Hooijer, A. *et al.* Current and future CO₂ emissions from drained peatlands in Southeast Asia. *Biogeosciences* **7,** 1505–1514 (2010).
24. Grace, J., Mitchard, E. & Gloor, E. Perturbations in the carbon budget of the tropics. *Glob. Change Biol.* **20,** 3238–3255 (2014).
25. Joosten, H. *The Global Peatland CO₂ Picture: Peatland Status and Emissions in All Countries of the World* (Wetlands International, 2009).
26. Alsdorf, D. *et al.* Opportunities for hydrologic research in the Congo Basin. *Rev. Geophys.* **54,** 378–409 (2016).
27. Ingram, H. A. P. Size and shape in raised mire ecosystems: a geophysical model. *Nature* **297,** 300–303 (1982).
28. Jaenicke, J., Rieley, J. O., Mott, C., Kimman, P. & Siegert, F. Determination of the amount of carbon stored in Indonesian peatlands. *Geoderma* **147,** 151–158 (2008).
29. Dommain, R., Couwenberg, J. & Joosten, H. Development and carbon sequestration of tropical peat domes in south-east Asia: links to post-glacial sea-level changes and Holocene climate variability. *Quat. Sci. Rev.* **30,** 999–1010 (2011).
30. Page, S. *et al.* A record of Late Pleistocene and Holocene carbon accumulation and climate change from an equatorial peat bog (Kalimantan, Indonesia): implications for past, present and future carbon dynamics. *J. Quaternary Sci.* **19,** 625–635 (2004).
31. Lähteenoja, O., Ruokolainen, K., Schulman, L. & Oinonen, M. Amazonian peatlands: an ignored C sink and potential source. *Glob. Change Biol.* **15,** 2311–2320 (2009).
32. Zhou, L. *et al.* Widespread decline of Congo rainforest greenness in the past decade. *Nature* **509,** 86–90 (2014).
33. Wetlands International. *Peta Sebaran Lahan Gambut, Luas dan Kandungan Karbon di Kalimantan/Maps of Area of Peatlands Distribution and Carbon Content in Kalimantan 2000–2002* (Wildlife Habitat Canada, 2004).

METHODS

Study area description. For logistical reasons the search for possible peat deposits was restricted to the Likouala Department, northern ROC. The Likouala Department covers 66,000 km^2, with most of the 154,000 population[34] living along the two main rivers of the region, the black-water Likouala-aux-herbes River and the white-water Ubangui River[35]. The region is almost entirely forested, of which the vast majority is swamp forest[9]. *Terra firme* forest is confined to narrow strips along river levees and the northwest of the region; savanna is found bordering the Likouala-aux-herbes River and surrounding villages and towns[9]. The underlying geology is Quaternary alluvium[35], and relief very gently sloping[35]. Rainfall is determined by the migration of the Intertropical Convergence Zone, which creates two wet and two dry seasons (major wet season, September to November; minor wet season, March to May[36]). The mean annual precipitation from the department capital, Impfondo, is 1,723 mm yr^{-1} (measured 1932–2007; ref. 36) and the mean annual temperature is 25.6 °C (measured 1950–1998; ref. 37).

Prospecting for peat. We searched for published records that identified locations of peat accumulation anywhere in the Cuvette Centrale. Although peat presence was noted by several sources, none provided geo-references or other identifying landscape features to allow us to confirm the presence of peat[10–13]. We therefore used theory and remotely sensed data to guide our search. Seven remote-sensing products were used to identify likely locations of peat accumulation, that is, locations with year-round waterlogging and overlying vegetation to provide organic matter inputs. The products are listed in Extended Data Table 1, with detailed information in Supplementary Methods.

Sites were selected to fully span the region, have an access point (one of the two major rivers), and traverse more than one vegetation type (Fig. 1). Sites included vegetation thought not to be associated with peat presence, thereby providing ground points from a wide range of vegetation types, which would later be used in the classification of remotely sensed imagery. Transects running perpendicular to the white-water Ubangui River (Bondzale, Ekolongouma, Mbala and Moungouma) and black-water Likouala-aux-herbes River (Bondoki, Ekondzo, Itanga and Makodi) allowed hypotheses about the role of river flooding and nutrient inputs from the two river systems to the peatlands to be tested: whether the Ubangi, with its higher banks, contributes substantial amounts of water to nearby swamps; and, if so, whether such locations with higher nutrient inputs may have higher decomposition rates and therefore no peat. The transect that reached the mid-point between the two rivers (Center) was chosen to assess whether peatlands extend fully across the large interfluvial area between the two rivers. The Moungouma transect, which crossed a series of old meanders of the Ubangi River, was not predicted to contain peat owing to the suspected high nutrient inputs from the Ubangi River, which was thought to lead to higher rates of organic matter decomposition. Transects were visited between January 2012 and May 2014.

Data collection. The length (2.5–20 km) and orientation of each transect were predetermined before arrival in the field, and were chosen on the basis of the likely logistical constraints and the hypotheses being investigated. Data collection was usually undertaken every 250 m along each transect following one of two protocols:

(1) Rapid protocol. This protocol was repeated every 250 m along each transect, except every 1,000 m when the full protocol occurred. The following data were collected. Peat thickness was measured by inserting metal poles into the ground until the poles were prevented from going any further by the underlying mineral layer[29,32]. Tree height measurements of five trees forming the canopy (top leaves fully exposed to the sun) were made using a laser hypsometer (Nikon Forestry Laser 550A S). Vegetation type and dominant species were also recorded.

(2) Full protocol. This protocol was repeated every 1,000 m along each transect (exceptions were the Center transect, for which the protocol was repeated every 4 km owing to the 20-km length of this transect; the Makodi transect, for which the protocol was repeated every 200 m owing to seemingly high spatial variation in vegetation communities; and the Moungouma transect, where sampling was irregular to ensure sampling captured both ridge and swale). At each location a complete peat core was extracted (52-mm Eijkelkamp Russian-type corer), subsampled in the field to 10-cm length, and sealed in plastic (see Methods section 'Peat sample analysis'). Groundwater or surface-water pH was measured (Hanna Instruments HI9124 Portable pH Meter), except at non-flooded non-peat sites where the water table was not accessible. A 20 m × 40 m plot was installed, with tree diameter and identity recorded for all trees with diameters of ≥10 cm diameter at 1.3 m along the stem, unless stilt roots, buttresses or a deformity was present, in which case the measurement was taken 30 cm above the non-cylindrical section of stem. The heights of five canopy trees (top leaves fully exposed to the sun), vegetation type and dominant species were also recorded identically to the rapid protocol.

Peat sample analysis. Sixty-one complete peat cores were transported to the UK for analyses. The organic matter content of samples (% by mass) was estimated using loss on ignition (LOI; 4 h, 550 °C). Samples that did not fit our definition of peat (depth of ≥0.3 m, organic matter content of ≥65%) were excluded from further analyses. For 2 of the 61 cores, the organic matter content had an intrusion of non-peat (organic matter content of <65%) part-way down the core, which we considered a mineral intrusion (affecting 20 cm and 30 cm of the two cores, respectively) rather than the base of the peat profile. The base of the peat core was defined as the point at which organic matter content decreased below 65% and remained so down the core.

To calibrate the metal pole method (rapid protocol) with the LOI method of determining peat depth (full protocol), both methods were undertaken at 24 of the 61 locations where a full core was extracted, with locations spanning the minimum to maximum peat depths. The two methods were strongly correlated ($P < 0.001$, adjusted $R^2 = 0.97$), and were used to calibrate all pole-only measurements (Extended Data Fig. 3).

To estimate the bulk density of the peat, samples of a known volume were dried at 105 °C for 24 h. Bulk density (ρ, in g cm^{-3}) was then calculated as $\rho = M/V$, where M is the mass (in g) of the sample and V is the volume (in cm^{-3}; from the corer dimensions) of the peat core section. Peat carbon concentration was estimated using an elemental analyser (EuroVector EA3000 Elemental Analyser).

Radiocarbon dating. Nine basal peat samples were radiocarbon dated (NERC Radiocarbon Facility, East Kilbride, Scotland), one each from the seven peatland sites sampled by the end of 2013, and two additional basal dates from different cores spanning the Ekolongouma transect (Extended Data Table 2). For two of the three Ekolongouma cores, two additional down-core peat samples were radiocarbon dated, and for the third, deepest core, nine additional down-core peat samples were radiocarbon dated (Extended Data Table 2). Further details of the radiocarbon-dating methods are given in Supplementary Methods.

Water-table levels. Continuous peatland water-table measurements, collected every 20 min for at least 12 months, were recorded via 12 below-ground pressure transducers (Solinst Levelogger Edge) installed across the Bondoki, Bondzale, Ekolongouma and Itanga transects. Additionally, above-ground pressure transducers (Solinst Barologger Edge) were installed, no more than 1 km from the below-ground transducers, to measure atmospheric pressure. The below-ground pressure transducers record a combination of water and atmospheric pressure; consequently, water pressure and thereby water-table levels were obtained by subtracting atmospheric pressure (using Solinst Levellogger Software, version 4).

The water-table data were inspected for flood events, but none was found (Extended Data Fig. 1), and compared to daily TRMM 3B42 satellite rainfall estimates (Tropical Rainfall Measuring Mission, 0.25° resolution, from http://giovanni.gsfc.nasa.gov/giovanni/). Monthly rainfall data comparisons require the monthly cumulative increase in water table (CIWT) to be calculated, the methods for which are given in Supplementary Methods.

Peatland surface topography. We wished to survey the surface topography of the peatlands, specifically to determine whether the peatlands are domed (as expected from rain-fed peatlands[27]). Without aircraft LiDAR, or *in situ* data from a differential GPS, we used satellite Digital Surface Model (DSM) data to create a Digital Terrain Model (DTM) by subtracting our *in situ* tree height data. We selected two transects, Itanga and Center, because they are contiguous (although follow different bearings: N 77° E and S 78° W, respectively) and extend from the peatland edge to the centre of one of the large interfluvial regions within the Cuvette Centrale. We used two satellite products to create two DTM products. First, we extracted the surface elevation of all pixels along the two transects from the ASTER Global Digital Elevation Map (GDEM; version 2) 30-m-resolution data for 2010[38]. Because this measures the top of forest canopies (it is a DSM), we obtained a ground surface (a DTM) by subtracting the maximum tree height estimate, that is, the tallest of our five *in situ* canopy tree height measurements sampled every 250 m along each transect.

The ASTER dataset is known to be noisy and susceptible to artefacts due to cloud cover, because it is created from optical images looking at two angles separated in time by about a minute, during which time clouds can move[39]. Therefore, second, we also calculated a second DTM from the SRTM 1-arc second-resolution data from 2000 for comparison[40]. This product sees a point about 30% into the vegetation; consequently, we subtracted the mean tree height of the five canopy trees sampled every 250 m along the transects. Neither technique revealed any obvious doming (Fig. 2). Our likely detection limits are domes of 3 m, with 5-m domes seen using similar techniques in southeast Asia[28]. We also looked for any evidence of domes in the raw DSM data, in the event that ground topography was discernible through the canopy surface topography. None was visible.

Peatland area estimates. Peatland area was estimated using a maximum likelihood classification of remotely sensed data that was trained and tested using ground-truth points to give estimates of the extent of land-cover classes across the Cuvette

Centrale, some of which are associated with peat. Five land cover classes were used in the classifications: *terra firme*, hardwood swamp, palm-dominated swamp, savanna and water (Extended Data Table 4). These classifications are based on seven land-cover classes observed in the field, because '*terra firme*' incorporates two vegetation types: seasonally flooded forest and *terra firme* forest, which were not easily distinguishable from each other via remote-sensing products (such differentiation was not necessary for this analysis because neither vegetation type overlies peat). 'Palm-dominated swamp' also incorporates two vegetation types: one dominated by *Raphia laurrentii* and another, rarer type dominated by *Raphia hookeri*, which were not easily distinguishable via remote-sensing products (again such differentiation was not necessary for this analysis because both overlie peat; Extended Data Table 4).

Of the five land-cover classes used, two were observed in the field to be strongly associated with the presence of peat: hardwood swamp forest and palm-dominated swamp forest (Extended Data Table 4). Hardwood swamp forest was consistently found to be associated with the presence of peat. Likewise, *Raphia laurentii* palm-dominated swamp forest was also consistently found to be associated with the presence of peat, whereas the much rarer *Raphia hookeri* palm-dominated swamp forest was found to be associated with the presence of channels or fluvial features, which often, but not always, contained peat (9 out of 17 on-the-ground sample points for *Raphia hookeri* palm-dominated swamp overlay peat). Therefore, although the palm-dominated swamp class is assumed to denote the presence of peat, it probably also represents very small areas of swamp that do not contain peat. Conversely, we assume that savanna does not generally overlie peat (only 1 of 12 on-the-ground sample points overlay peat, in this case a sample point within a seasonal stream).

Ground-truth data to train the classification algorithm, and to assess the accuracy of the output classification, were collected using a GPS (Garmin GPSmap 60CSx) from our study region (250 points from all land-cover classes) and far from our study sites in DRC (28 *terra firme* with no peat, 5 for hardwood swamp sites with peat (observed peat depths at these points were 0.9 m, 1.6 m and, at three locations, >2 m depth)), and via Google Earth for unambiguous, non-peat classes only: savanna (59 points), *terra firme* (77 points) and water (69 points).

Eight products, similar to those used to locate the field sites, were used to map the five land-cover classes, including radar, optical and DEM-derived data (three ALOS PALSAR, two SRTM-derived variables and three Landsat ETM+ bands; see Extended Data Table 5).

A supervised maximum likelihood classification was run 1,000 times using IDL-ENVI, using a jack-knife approach to select different combinations of training and test plots for each run, to produce a consensus classification with a spatial assessment of uncertainty. Maximum likelihood was chosen because the accuracies of initial maximum likelihood classifications were higher than classifications using other commonly used techniques (we tested minimum distance, Mahalanobis distance, neural networks and support vector machine algorithms). To reduce computation time, principal component analysis was used to reduce the eight remote-sensing datasets to six uncorrelated principal components that were then used in the maximum likelihood classifications. For each of the 1,000 classification iterations, two-thirds of the ground-truth points from each class were randomly selected for use as training data. Each iteration produced a land-cover classification for each pixel and therefore an area estimate for each land-cover class. Thus, there were 1,000 estimates for each pixel of its land-cover class, which we express as a percentage probability of the most commonly allocated class (Fig. 1). Our best estimate of peatland area is the median value of the combined palm-dominated swamp and hardwood swamp areas from each of the 1,000 runs, alongside the 95% CI (2.5th and 97.5th percentile). The random selection of one-third of the points retained as independent test data in each run were then used to estimate the accuracy of that run. This procedure, repeated 1,000 times, gives the user's and producer's accuracy of each land-cover class, and an overall classification accuracy (see Extended Data Table 6).

Below-ground carbon stocks. The peatland below-ground carbon (BGC) stock was assessed by multiplying the peatland area from the maximum likelihood classification and the estimated carbon storage per unit area derived from peat depth, bulk density and carbon concentration measurements. We found no evidence of a difference in peat depth, bulk density or carbon concentration between the palm-dominated swamp and hardwood swamp areas, so we simply sum the two classes. To calculate the carbon stocks per unit area (core depth × bulk density × carbon concentration), we first used 44 cores of known depth for which we had estimates of bulk density and carbon concentration. Estimates of carbon storage of each 0.1-m depth of each core were summed to provide an estimate of carbon storage for each core (in Mg C ha^{-1}). Bulk density measurements were usually taken every other 0.1 m down each core, so interpolation was used for missing data. Because bulk density was highly variable down-core,

only the 44 well-sampled cores were included. For carbon concentration, 12 cores had been sampled every other 0.1 m, and we interpolated the missing values. However, carbon concentration variability was low among cores (Table 1), and a regular pattern with depth was seen: an increase to a depth of about 0.5 m, followed by a long, very weak decline, and finally a strong decline over the deepest approximately 0.5 m of the core. For the 12 well-sampled cores, we used segmented regression (*segmented* package in R, version 0.5-1.4) to parameterize the three sections of the core, using the means of these relationships to interpolate the carbon concentration for each 0.1-m depth for the remaining 32 cores that had less-intensive carbon concentration sampling. Second, we used the relationship of total core depth and per-unit-area carbon stocks of the 44 cores (Extended Data Fig. 3) to estimate carbon stocks from all 211 measurements of peat depth across the study area.

We used a resampling approach to estimate uncertainty, by randomly selecting a measured peat depth, calculating the per-unit-area carbon stocks, including the uncertainty associated with the depth–carbon stocks relationship, and then multiplying this by a randomly selected total peatland area, to give the total BGC stock, expressed in petagrams. We first bootstrapped the measurements of peat depth, the uncertainty on the depth–carbon stocks relationship, and the peatland area, trimming at the 2.5th and 97.5th percentile values[41]. We then randomly selected a depth, depth–carbon stock intercept and corresponding slope, and a total peatland area, and repeated this, with replacement, 100,000 times, reporting the median as the best estimate and 95% CI as the 2.5th and 97.5th percentiles (Extended Data Fig. 4). This procedure avoids occasional unrealistic (negative) BGC estimates derived from shallow depths combining with the uncertainty associated with the depth–carbon stock relationship. Details of how we integrated our new estimates into pan-tropical estimates of peat carbon stocks are given in Supplementary Methods.

Above-ground carbon stocks. Above-ground carbon (AGC) stocks were estimated using 60 40 m × 20 m vegetation plots installed every 1 km along each transect (Makodi transect, every 200 m; Center transect, every 4 km), and using allometric equations[42–44], including diameter, wood density and tree height[45], assuming 47% carbon content[46]. Wood specific gravity values were taken from the Global Wood Density Database[47,48]. The AGC stock of each plot is the sum of the AGC stocks for each individual stem, expressed as Mg C ha^{-1}. Mean AGC was higher in the hardwood swamp (123.6 Mg C ha^{-1}; 95% CI, 105.5–145.2 Mg C ha^{-1}; $n = 25$) than in the palm-dominated swamp (67.0 Mg C ha^{-1}; BCa 95% CI, 51.9–86.4 Mg C ha^{-1}; $n = 35$). Full details are given in Supplementary Methods.

Total AGC stock across the swamps of the Cuvette Centrale was calculated using a resampling method. We randomly sampled, with replacement, one run of the maximum likelihood classification, and extracted the extent of peatland in palm-dominated swamp and the corresponding extent of peatland in hardwood swamp from that run. We then randomly selected, with replacement, an AGC value for palm-dominated swamp and an AGC value for hardwood swamp, and multiplied them by their corresponding areas from the single maximum likelihood run. We then summed them to obtain an estimate of the total peatland AGC stocks. We repeated this 10,000 times, reporting the median, mean and 95% CI, as the 2.5th and 97.5th percentiles.

Data availability. The data that support the findings of this study are available from the corresponding author upon request. The peatland probability map for the Cuvette Centrale (Fig. 1c), as a raster file, is publicly available from the African Tropical Rainforest Observation Network (AfriTRON), http://www.afritron.org/en/peatland.

The datasets cited in Extended Data Table 1 are available from http://www.eorc.jaxa.jp/ALOS/en/kc_mosaic/kc_map_50.htm (ALOS PALSAR 50-m Orthorectified Mosaic) and http://earthexplorer.usgs.gov/ (Landsat ETM imagery and SRTM DEM 3-arcsecond, void-filled data). The datasets cited in Extended Data Table 5 are available from http://www.eorc.jaxa.jp/ALOS/en/palsar_fnf/data/index.htm (ALOS PALSAR 50-m HH and HV data), http://earthexplorer.usgs.gov/ (SRTM DEM 1-arcsecond data and ASTER GDEM, version 2, 1-arcsecond data) and http://osfac.net/ (OSFAC ROC and DRC Landsat ETM+ bands 5, 4 and 3 mosaics).

34. Centre Nationale de la Statistique et des Etudes Economiques du Congo. *Population des Départements- Likuoala* http://www.cnsee.org/index.php?option=com_content&view=article&id=135%3Apopdep&catid=43%3Aanalyse-rgph&Itemid=37&limitstart=9 (accessed 25 May 2016).
35. Laraque, A., Bricquet, J. P., Pandi, A. & Olivry, J. C. A review of material transport by the Congo River and its tributaries. *Hydrol. Processes* **23**, 3216–3224 (2009).
36. Samba, G. & Nganga, D. Rainfall variability in Congo-Brazzaville: 1932–2007. *Int. J. Climatol.* **32**, 854–873 (2012).

37. Samba, G., Nganga, D. & Mpounza, M. Rainfall and temperature variations over Congo-Brazzaville between 1950 and 1998. *Theor. Appl. Climatol.* **91,** 85–97 (2008).
38. NASA/METI. *The Advanced Spaceborne Thermal Emission and Reflection Radiometer (ASTER) Global Digital Elevation Model (GDEM) version 2* http://earthexplorer.usgs.gov/ (2011).
39. Tachikawa, T. *et al. ASTER Global Digital Elevation Model Version 2 - Summary of Validation Results* (NASA, 2011).
40. USGS. *Shuttle Radar Topography Mission (SRTM) 1 arc-second Digital Elevation Model (DEM)* http://earthexplorer.usgs.gov/ (2006).
41. Keselman, H. J., Wilcox, R., Othman, R. & Fradette, A. R. K. Trimming, transforming statistics, and bootstrapping: circumventing the biasing effects of heterescedasticity and nonnormality. *J. Mod. Appl. Stat. Methods* **1,** 38 (2002).
42. Lewis, S. L. *et al.* Above-ground biomass and structure of 260 African tropical forests. *Phil. Trans. R. Soc. Lond. B* **368,** 20120295 (2013).
43. Feldpausch, T. R. *et al.* Tree height integrated into pantropical forest biomass estimates. *Biogeosciences* **9,** 3381–3403 (2012).
44. Goodman, R. C. *et al.* Amazon palm biomass and allometry. *For. Ecol. Manage.* **310,** 994–1004 (2013).
45. Chave, J. *et al.* Improved allometric models to estimate the aboveground biomass of tropical trees. *Glob. Change Biol.* **20,** 3177–3190 (2014).
46. Martin, A. R. & Thomas, S. C. A reassessment of carbon content in tropical trees. *PLoS One* **6,** e23533 (2011).
47. Zanne, A. E. *et al. Data from: Towards a Worldwide Wood Economics Spectrum* http://dx.doi.org/10.5061/dryad.234 (Dryad Digital Repository, 2009).
48. Chave, J. *et al.* Towards a worldwide wood economics spectrum. *Ecol. Lett.* **12,** 351–366 (2009).
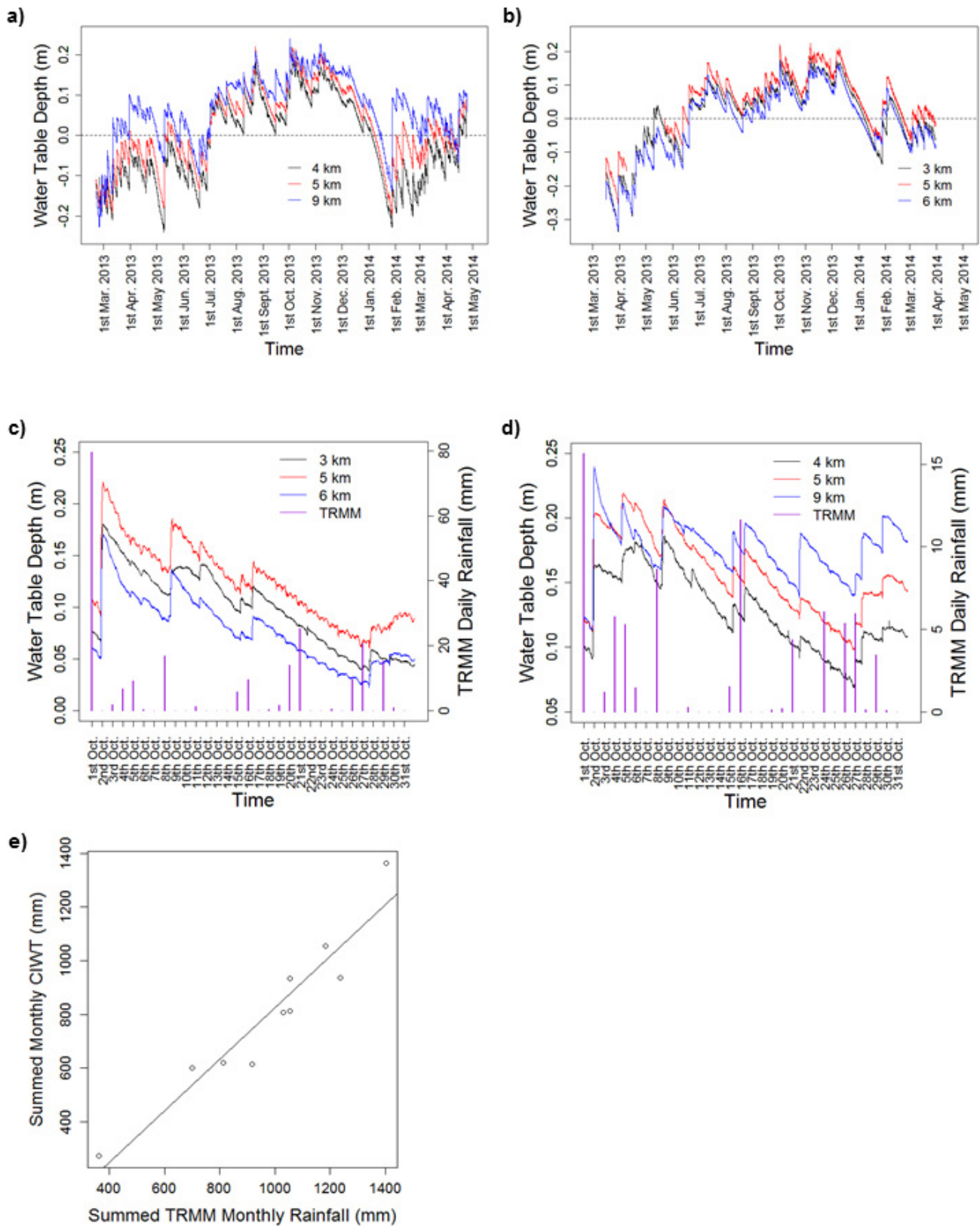
Extended Data Figure 1 | Peatland water table time-series data.
**a**, **b**, Time series of water-table levels for the Ekolongouma (**a**) and Itanga (**b**) transects for the time period March 2013 to May 2014 (black, blue and red lines indicate different sample locations along the transects). **c**, **d**, Time series of water-table levels for the wet-season month of October 2013 for the Ekolongouma (**c**) and Itanga (**d**) transects, when river-caused flood events are more likely (left-hand axis; black, blue and red lines), and daily TRMM rainfall estimates (right-hand axis; purple lines). No obvious flood waves are seen. **e**, Relationship between the summed monthly cumulative increase in water table (CIWT) from 10 pressure transducers (Itanga,

Ekolongouma, Bonzale and Bondoki transects), for months in which CIWT > 0, and summed monthly rainfall estimates for the same months from TRMM (best-fitting line: $y = 0.959x - 133$, $R^2 = 0.90$, $P < 0.001$). Months during which the water table was not always above the peatland surface (CIWT ≤ 0) were excluded from the analysis, owing to large changes in the water table that obscure the relationship between water table and water input. Data from 10 pressure transducers are included, because two transducers had no months during which the water table was consistently above the peat surface.
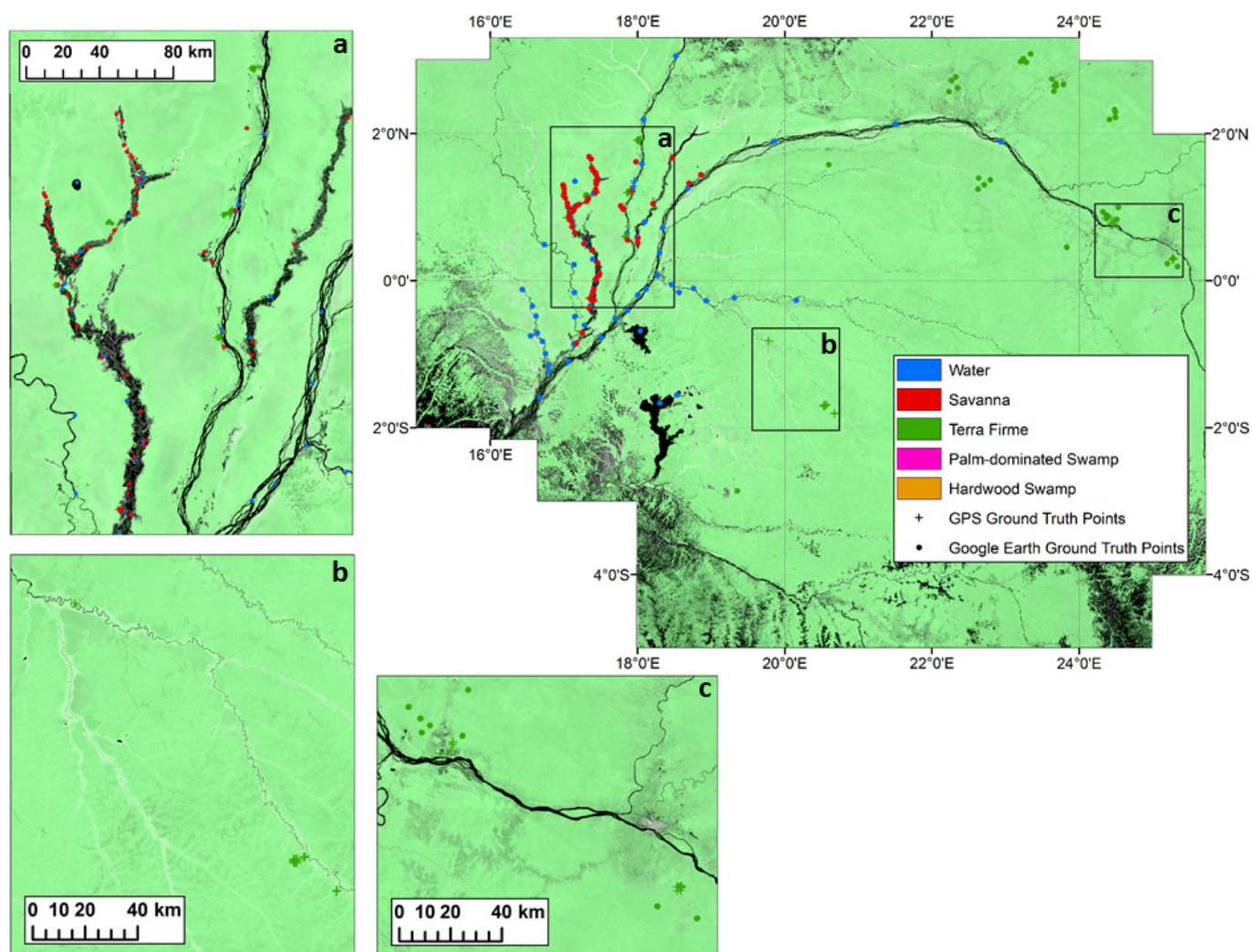
Extended Data Figure 2 | Spatial distribution of the ground-truth points across the Cuvette Centrale. Main panel, ALOS PALSAR imagery of the Cuvette Centrale area and the spatial distribution of the ground-truth points (crosses for GPS, circles for Google Earth derived points) that were used as test and training data in the 1,000 runs of the maximum likelihood classifications used to estimate regional peat extent. The black boxes correspond to the other panels: **a**, the main study region; **b, c**, two regions within DRC where GPS ground-truth points were also obtained.

a)

b)
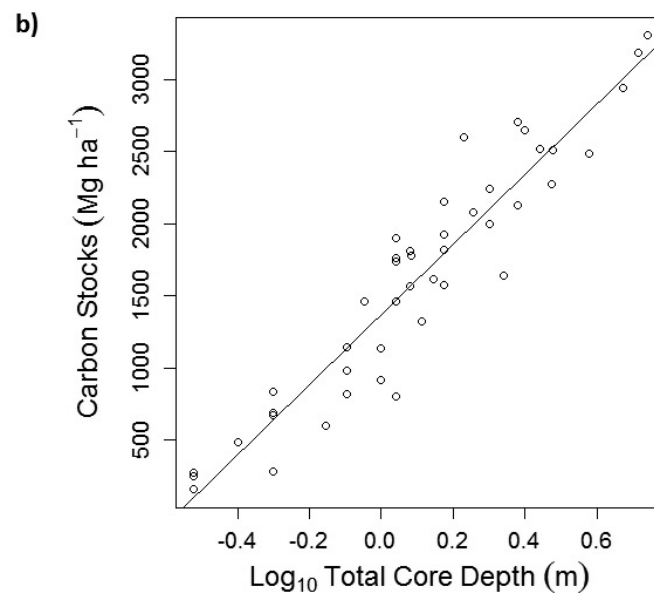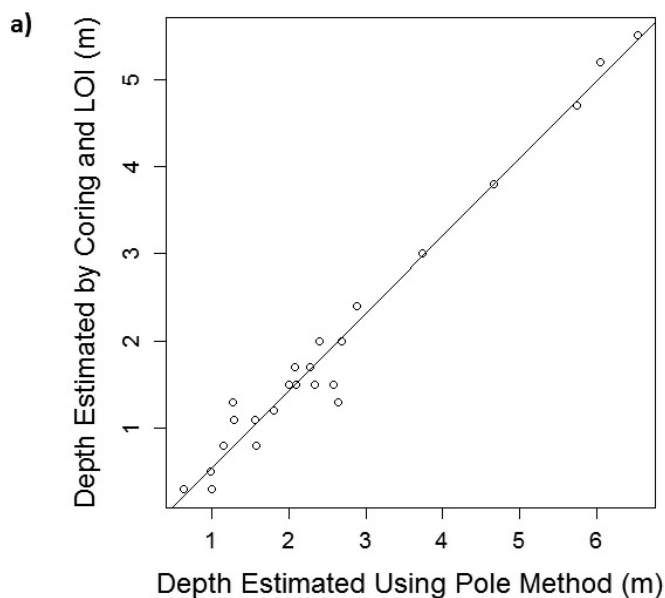
Extended Data Figure 3 | Relationship between estimates of peat depth using the field-pole method and those using peat cores followed by laboratory analysis, and the relationship between corrected peat depth and total peat carbon stocks. a, Relationship between peat depth (in m) estimated using a metal pole (rapid protocol) and estimated using coring and laboratory analysis (full protocol); LOI, loss-on-ignition; best-fitting line: $y = 0.888x - 34.8$, $R^2 = 0.97$, $P < 0.001$, where y is cored peat depth and x is pole peat depth. The organic matter content of the core must be $\geq 65\%$ to be classified as peat. Soft carbon-rich material that is $<65\%$ organic matter is captured using the rapid protocol, which lies beneath peat using our definition, but above the more typical mineral soil. **b**, Relationship between core depth (in m) and total carbon stocks (in Mg C ha^{-1}) for cores from the Cuvette Centrale (best-fitting line: carbon stocks $= 1,374 + 2,425\log_{10}$(total core depth), $R^2 = 0.89$, $P < 0.0001$).
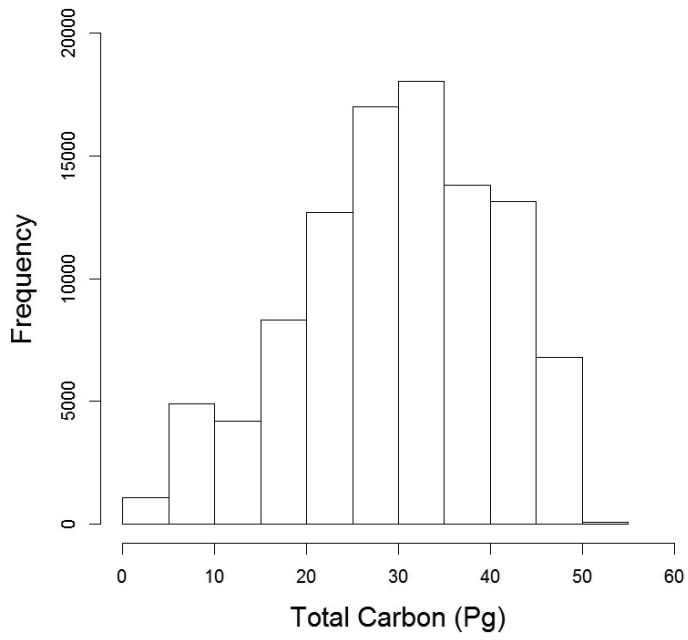
Extended Data Figure 4 | Distribution of peatland carbon stock estimates. Estimated carbon stocks from 100,000 resamples of peatland area, peat depth and per-unit-area carbon storage. Median, 30.6 Pg C; mean, 29.8 Pg C; 95% CI, 6.3–46.8 Pg C.

Extended Data Table 1 | Description of remote-sensing products used to identify field sites in the Cuvette Centrale

Product	Spatial Resolution	Acquisition Date	Product Description	Data Provider and Repository	Detection Capability
ALOS PALSAR* 50 m Orthorectified Mosaic Product	50 m	Sep. 2007 to Jun. 2009	Both polarised (HH)‖ and cross polarised (HV)¶ imagery used in a HH-HV-HH red, green, blue display.	JAXA EORC (http://www.eorc.jaxa.jp/ALOS/en/kc_mosaic/kc_map_50.htm)	Differentiates areas of inundated forest from non-flooded forest, as well as forest vs. non-forest.
RFDI†	50 m	Sep. 2007 to Jun. 2009	Created from a PALSAR HH and HV product. RFDI is the polarization ratio of (HH - HV) / (HH + HV), used to exaggerate polarisation differences for each pixel independent of total backscatter.	JAXA EORC (http://www.eorc.jaxa.jp/ALOS/en/kc_mosaic/kc_map_50.htm)	Differentiates areas of inundated forest from non-flooded forest.
SRTM DEM‡	~90 m	Feb. 2000	3-arc second version, void-filled.	USGS (http://earthexplorer.usgs.gov/)	Detects depressions in landscape where water could accumulate, and/or shorter or a more open vegetation canopy, all possibly linked to wetland vegetation.
Landsat ETM§	30 m	18th Feb. 2001	Bands 4, 5 and 7 displayed as red, green and blue respectively.	NASA/USGS (http://earthexplorer.usgs.gov/)	Detects different vegetation classes.

*Advanced Land Observation Satellite (ALOS) Phased Array type L-band Synthetic Aperture Radar (PALSAR).
†Radar Forest Degradation Index (RFDI).
‡Shuttle Radar Topography Mission (SRTM) Digital Elevation Model (DEM).
§Landsat Enhanced Thematic Mapper (ETM+).
‖HH, radar signal that is transmitted and detected in a horizontal (H) polarization.
¶HV, radar signal that is transmitted in a horizontal (H) polarization, but detected in a vertical (V) polarization.

Extended Data Table 2 | Radiocarbon dates from nine peat cores

Site	Sample Code	Distance Along Transect (km)	Depth (m)	¹⁴C Age	Error (1σ)	δ ¹³C	Calibrated Age (cal yrs BP) (2σ)	
							Median	Range
Bondoki	SUERC-56866	6	1.40-1.50	7352	38	-30.0	8169	8033-8216 8242-8253 8256-8304
Bondzale	SUERC-57586	6	1.60-1.70	6817	39	-25.1	7647	7585-7708
Ekolongouma	SUERC-49356	4	0.57-0.60	2649	37	-31.0	2792	2739-2808
Ekolongouma	SUERC-49357	4	1.07-1.10	7652	42	-29.7	8464	8389-8524 8527-8538
Ekolongouma	SUERC-49358	4	1.47-1.50	8484	41	-29.6	9494	9450-9537
Ekolongouma	SUERC-49351	7	0.57-0.60	2547	37	-31.1	2623	2493-2599 2609-2639 2680-2752
Ekolongouma	SUERC-49354	7	1.17-1.20	7600	38	-29.9	8401	8348-8453
Ekolongouma	SUERC-49355	7	2.37-2.40	9091	39	-21.8	10281	10190-10297 10329-10340 10355-10372
Ekolongouma	SUERC-49348	9	0.57-0.60	1571	35	-30.1	1464	1389-1539
Ekolongouma	SUERC-56133	9	0.67-0.70	1754	38	-30.5	1684	1562-1740 1756-1781 1798-1806
Ekolongouma	SUERC-56134	9	0.77-0.80	1720	35	-29.4	1632	1556-1707
Ekolongouma	SUERC-56135	9	0.87-0.90	702	36	-29.7	628	561-595 635-694
Ekolongouma	SUERC-49349	9	0.97-1.00	4811	37	-31.1	5538	5470-5561 5567-5606
Ekolongouma	SUERC-56138	9	1.27-1.30	4251	37	-29.7	4760	4649-4672 4699-4759 4807-4870
Ekolongouma	SUERC-56139	9	1.67-1.70	6354	39	-29.4	7296	7176-7218 7239-7337 7352-7416
Ekolongouma	SUERC-56140	9	1.97-2.00	7662	39	-29.0	8469	8398-8539
Ekolongouma	SUERC-56141	9	2.37-2.40	7993	40	-29.3	8835	8663-8666 8716-9007
Ekolongouma*	SUERC-49350	9	2.70-2.73	9340	41	-29.6	10554	10428-10465 10481-10679
Ekondzo†	*SUERC-56868*	*5*	*2.10-2.20*	*2147*	*35*	*-30.0*	*2155*	*2005-2027 2036-2183 2199-2203 2234-2305*
Itanga	SUERC-56869	6	1.90-2.00	8575	46	-26.6	9566	9481-9629 9649-9651
Makodi	SUERC-56870	NA‡	1.17-1.20	6239	39	-30.3	7137	7017-7125 7149-7257
Mbala	SUERC-56873	6	2.40-2.50	7765	38	-30.2	8525	8446-8604

*The deepest approximately 25 cm of peat profile could not be recovered. This is the deepest sample recovered. On the basis of the average peat accumulation rate for this core (0.26 mm yr⁻¹; Extended Data Table 3), peat initiation could have commenced about 960 years earlier at this location, around 11,500 cal yr BP.
†The Ekondzo basal sample date is considered an erroneous outlier, due to possible contamination with younger carbon, and is not reported in the main text (see Supplementary Methods).
‡The deepest peat core from the Makodi site was sampled off transect (400 m N 41° W from the transect) and so there is no corresponding transect distance for this sample.

Extended Data Table 3 | Average peat accumulation rate and long-term rate of carbon accumulation (LORCA) for nine radiocarbon-dated peat cores

Site	Distance Along Transect (km)	Depth (m)	Time Period (cal yrs BP)	Accumulation Rate (mm yr^{-1})	LORCA (g C m^2 yr^{-1})
Bondoki	6	1.40-1.50	8169 to -63	0.18	18.30
Bondzale	6	1.60-1.70	7647 to -63	0.21	32.88
Ekolongouma	4	1.47-1.50	9494 to -62	0.16	19.95
Ekolongouma	7	2.37-2.40	10281 to -62	0.23	22.80
Ekolongouma	9	2.70-2.73	10554 to -62	0.26	20.45
*Ekondzo**	*5*	*2.10-2.20*	*2155 to -63*	*0.97*	*67.95*
Itanga	6	1.90-2.00	9566 to -63	0.20	22.94
Makodi	NA‡	1.17-1.20	7137 to -63	0.16	21.08
Mbala	6	2.40-2.50	8525 to -63	0.29	33.10

*The much higher accumulation rate and LORCA from the Ekondzo core is considered an error, due to the exceptionally young basal radiocarbon date from this core, and is not reported in the main text (see Supplementary Methods).
‡The deepest peat core from the Makodi site was sampled off transect (400 m N 41° W from the transect) and so there is no corresponding transect distance for this sample.

Extended Data Table 4 | Vegetation classes encountered in the field, and their associations (or not) with peat

Vegetation Class	Description	Associated With Peat?
Terra firme Forest	Generally limited in extent within the swamp areas. Was most commonly found adjacent to the Ubangui River. Includes both primary and secondary vegetation. Dominated by dicots. Understorey frequently dominated by *Sarcophrynium* spp. (Marantaceae). Never or very rarely floods.	No
Seasonally Flooded Forest	Generally limited to occurring in transition zones between non-swamp (either savanna or *terra firme*) and swamp vegetation. Dominated by dicots. Lianas often very abundant and sometimes dominate. Topographically very variable on a small scale, with a system of mounds and channels. Understorey is often confined to the mounds. Species such as *Guibourtia demeusei* and *Dialium pachyphyllum* can often be found. Usually only floods in the major wet season.	No
Hardwood Swamp	Common within swamp areas. Dominated by dicots. Trees often showing adaptations to wet conditions such as stilt and aerial roots and buttresses. Species commonly found across all sites include *Uapaca paludosa, Carapa procera, Symphonia globulifera* and *Xylopia rubescens*. Myristicaceae spp. was often abundant in the sub-canopy.	Yes
Raphia laurentii Palm-dominated Swamp	Common within swamp areas. *Raphia laurentii* dominant or monodominant swamp. The *Raphia laurentii* is a trunkless palm with fronds reaching up to 12-14 m in length. A more open vegetation type than the hardwood swamp. Tree species present are the same as the hardwood swamp, but in much lower abundance. Ferns are often common in the understorey.	Yes
Raphia hookeri Palm-dominated Swamp	Rare in swamp areas. *Raphia hookeri* dominated. *Raphia hookeri* forms a trunk and reaches heights of up to ca. 16 m. It appears to be associated with the presence of seasonal channels or old fluvial features.	Yes, but not consistently, and, relative to the hardwood and *Raphia laurentii* palm-dominated swamp, not associated with thick peat deposits (max. peat depth 1.1 m).
Savanna	Largely limited to areas adjacent to major rivers and near villages. Grassland often dominated by *Hyparrhenia diplandra*. Seasonally flooded in parts. Seasonally burned. Boundary between savanna and forest is very abrupt.	No, except on a single occasion, where one shallow (0.3 m), discrete peat deposit was found beneath a savanna stream.

Extended Data Table 5 | Remote-sensing products used in the maximum likelihood classification to map peatland extent within the Cuvette Centrale

Product	Spatial Resolution	Acquisition Date	Product Description	Data Provider and Repository	Detection Capability
ALOS PALSAR* HV†	50 m	2007-2010	Mean PALSAR HV values from the years 2007-2010	JAXA EORC (http://www.eorc.jaxa.jp/ALOS/en/palsar_fnf/data/index.htm)	Differentiates high biomass from low biomass areas and/or open water.
ALOS PALSAR HH‡	50 m	2007-2010	Mean PALSAR HH values from the years 2007-2010	JAXA EORC (http://www.eorc.jaxa.jp/ALOS/en/palsar_fnf/data/index.htm)	Differentiates waterlogged forested areas from well-drained forested areas or open wetlands/non-wetland areas.
ALOS PALSAR HV/HH	50 m	2007-2010	HV/HH ratios created from the above mean PALSAR HV and HH mosaics.	JAXA EORC (http://www.eorc.jaxa.jp/ALOS/en/palsar_fnf/data/index.htm)	Differentiates between flooded and non-flooded forests.
SRTM DEM§	1-arc second resized to 50 m	2000	SRTM DEM with voids (i.e. extremely large negative numbers) present in the data filled using ASTER GDEM‖ (version 2) 1-arc second data.	SRTM: USGS (http://earthexplorer.usgs.gov/) ASTER: NASA and METI (http://earthexplorer.usgs.gov/)	Detects depressions where water may accumulate and/or shorter and/or a more open vegetation canopy, all possibly linked to wetland vegetation.
SRTM slope	1-arc second resized to 50 m	2000	Slope calculated from the above SRTM DEM using the Topographic Modelling tool in ENVI 4.6.1 and a 3x3 window.	SRTM: USGS (http://earthexplorer.usgs.gov/) ASTER: NASA and METI (http://earthexplorer.usgs.gov/)	Differentiates slopes, with high values likely associated with better drainage (non-swamp, often *terra firme* forest) and low values likely associated with inundation (often peatland areas) or water bodies.
Landsat ETM+¶ (bands 5,4,3)	60 m resized to 50 m	2005-2010	OSFAC ROC and DRC Landsat ETM+ (bands 5, 4 and 3) mosaics. Each band in the ROC mosaic is the median of the years 2000, 2005 and 2010 and a composite of the years 2005 to 2010 for the DRC.	OSFAC (http://osfac.net/)	Differentiates major vegetation types

*Advanced Land Observation Satellite (ALOS) Phased Array type L-band Synthetic Aperture Radar (PALSAR).
†HH, radar signal that is transmitted and detected in a horizontal (H) polarization.
‡HV, radar signal that is transmitted in a horizontal (H) polarization, but detected in a vertical (V) polarization.
§Shuttle Radar Topography Mission (SRTM) Digital Elevation Model (DEM).
¶Landsat Enhanced Thematic Mapper (ETM+).
‖Advanced Spaceborne Thermal Emission and Reflection Radiometer (ASTER) Global Digital Elevation Model (GDEM).

Extended Data Table 6 | Land-cover classes, ground-truth sample sizes, estimated extent of each class from 1,000 maximum likelihood model runs, and producer's, user's and overall accuracy of the classifications

Land Cover Class	Signifies Peat Presence?	Total No. of Ground Truth Points	No. of GPS Ground Truth Points	No. of Google Earth Ground Truth Points	Median Producer's Accuracy (%) (95% CI)	Median User's Accuracy (%) (95% CI)	Median Estimated Extent (km²) (95% CI)
*Terra firme**	No	144	61	83	71 (60-81)	89 (79-97)	772,400 (751,000-786,800)
Hardwood swamp	Yes	129	129	0	77 (65-88)	62 (54-71)	79,042 (68,100-90,500)
Palm-dominated swamp†	Yes	101	101	0	69 (53-82)	75 (63-88)	66,300 (56,900-74,700)
Total Swamp‡	Yes	230	230	0	94 (88-99)	84 (80-90)	145,500 (131,900-156,400)
Savanna	No	66	14	52	95 (86-100)	95 (84-100)	26,300 (20,900-35,400)
Water	No	76	3	73	96 (88-100)	96 (83-100)	35,000 (19,700-57,000)
Total	NA	516	311	205	Median Overall Classification Accuracy (95% CI) §: Separate swamp classes: 79 (74-84) Combined swamp classes: 88 (84-92)		NA

*Class includes both *terra firme* forest and seasonally flooded forest; see Extended Data Table 4 for descriptions.
†Class includes both *Raphia laurentii* and *Raphia hookeri* palm-dominated swamp; see Extended Data Table 4 for descriptions.
‡Hardwood swamp and palm-dominated swamp classes combined.
§For each of the 1,000 classifications, the overall classification accuracy was calculated as the percentage of test ground-truth points assigned to the correct class in the classification.